# Supplementary Information

# Temperature-cycle microscopy reveals single-molecule structural heterogeneity

Haifeng Yuan[a,†], Alexander Gaiduk[a], Joanna Siekierzycka[a], Satoru Fujiyoshi[b], Michio Matsushita[b], Daniel Nettels[c], Benjamin Schuler[c], Claus. A. M. Seidel[d] and Michel Orrit[a*]

[a]Huygens-KamerlingOnnes Laboratory, Leiden University, Leiden, The Netherlands. *E-mail: orrit@physics.leidenuniv.nl

[b]Department of Physics, Tokyo Institute of Technology, Tokyo, Japan.

[c]Department of Biochemistry, University of Zurich, Zurich, Switzerland

[d]Institute for Physical Chemistry, Heinrich-Heine-Universität Düsseldorf, Düsseldorf, Germany.

[†]Present address: Department of Chemistry, KU Leuven, Leuven, Belgium

## Optical alignment of the solid immersion lens.

The alignment of the SIL-objective system is achieved using the patterns (spherical disks/rings) of the back-reflected light on a CCD camera. Adjusting the in-plane position of the sample, on which the SIL is attached, one can achieve a symmetric spherical pattern only when the SIL and objective is well centered. Further approaching the sample towards the objective along the vertical direction will then focus the beam onto the SIL sample interface.

## Temperature cycles on gold nanorods in glycerol.

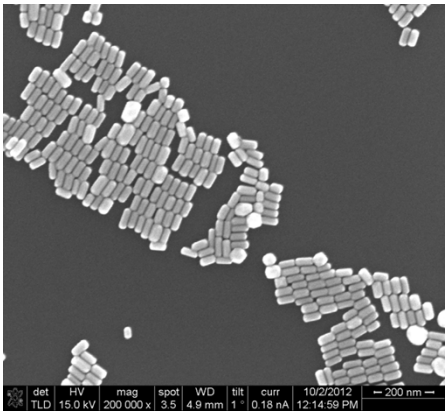


Fig. S1 SEM image on the gold nanorods (58±7 nm in length and 25±4 nm in diameter).

**Sample preparation:**

Gold nanorods were synthesised through the seed-mediated method[1] using cetyltrimethylammonium bromide (CTAB) as surfactant. The suspension of nanorods was centrifuged and washed several times to reduce the CTAB concentration to about 100 μM. Then 1 μL nanorod suspension was gradually added into 300 μL glycerol under stirring. Afterwards, the mixture was vortexed for 60 seconds. 100 μL of nanorod glycerol suspension was then dropped onto a clean substrate (Cr and $SiO_2$ coated) and was spin-casted using the same parameters as that used for single-molecule samples (6000 rpm for 90 seconds). A low-temperature objective (NA=0.82) was used in this experiment. A 633nm diode laser was used for excitation. Filters were changed accordingly.

**Results:**

The photoluminescence intensity traces recorded at different polarizations were shown in Fig. S2a. Each data point was taken after a temperature cycle between 228 K and 290 K. The photoluminescence intensities showed strong anti-correlation yielding a dynamic linear dichroism trace as in Fig.S2b, indicating the nanorod's in-plane orientation was evolving upon temperature cycles. However, after about 700 temperature cycles, the nanorod became immobile which is probably due to its attachment onto the substrate. Though the linear dichroism trace is not long enough for an autocorrelation study, we can estimate the average rotational duration to about 150 temperature cycles. Taking into account the 0.1 ms heating duration in each temperature cycle, the rotational time recovered from temperature-cycle measurement corresponds to about 15 ms, which is the expected rotational time for a 25 nm by 58 nm nanorod at 298 K. The expected rotational time for a 25 nm by 58 nm nanorod is 33 ms at 290 K[2], which is about twice slower than the value we measured. The difference may come from the

following several factors. (1) The volume distribution of the nanorods. (2) The measurement uncertainty in our previous heating calibration.[3, 4].

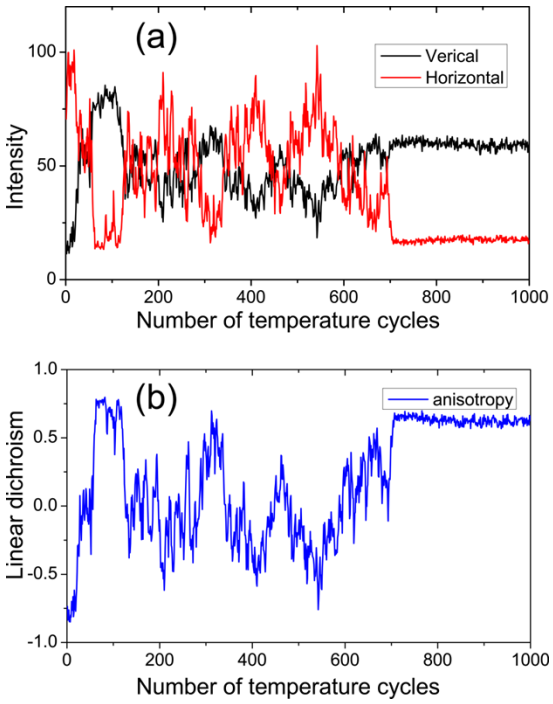


Fig. S2 (a) Photoluminescence trace at two polarizations from a single gold nanorod in glycerol under temperature cycles. The environmental temperature was 228 K. In each temperature cycle, the temperature around the nanorod was brought to 290 K for 0.1 ms. (b) The corresponding linear dichroism trace calculated from the trace shown in (a).

Therefore, by following the rotational dynamics of individual gold nanorods we can confirm that dynamics of objects inside our heating volume indeed evolve in the expected manner upon temperature cycles.

**Accesible volume calculation on the dsDNA sample.**

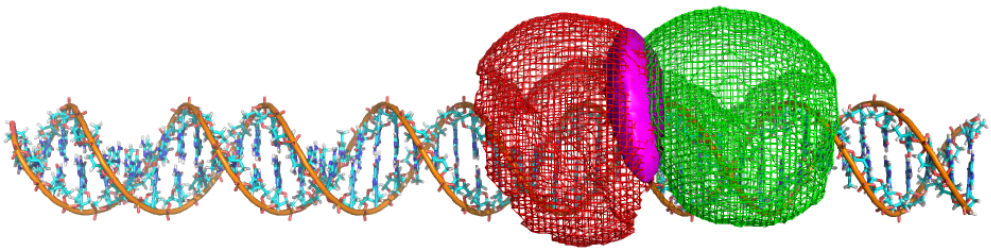

Fig. S3 The simulated accessible volumes of the donor dye (red) and the acceptor dye (green) of a FRET labeled dsDNA construct. The two dyes were labeled at a separation of 7 basepairs. The magenta points represent the volume in which the dye-dye distance is less than 0.5 nm.

A simulation on the accessible volumes of both dyes on a dsDNA construct was also carried out according to the method reported by Sindbert *et al.*.[5] The result is shown in Figure S3. Though the two dyes are separated with a distance of 7 DNA basepairs, there is a small volume (colored with magenta) in which the two dyes can be less than 0.5 nm to each other. When such short inter-dye separations occur, strong interactions can take place and can influence the FRET observed. Similarly, the very short inter-dye separations can also occur in polyproline constructs but more frequent due to the following several reasons. (1) The labeling positions on a polyproline construct are separated with 6 proline units, which is slightly shorter than that in a dsDNA construct. (2) There is less molecular structure that blocks the two dyes from getting closer to each other in polyproline constructs. Dye-dye interactions are thus likely to be more pronounced for our FRET-labeled polyproline constructs.

**Nanosecond fluorescence correlation spectroscopy on Pro6 and Pro20 in aqueous solution at room temperature.**

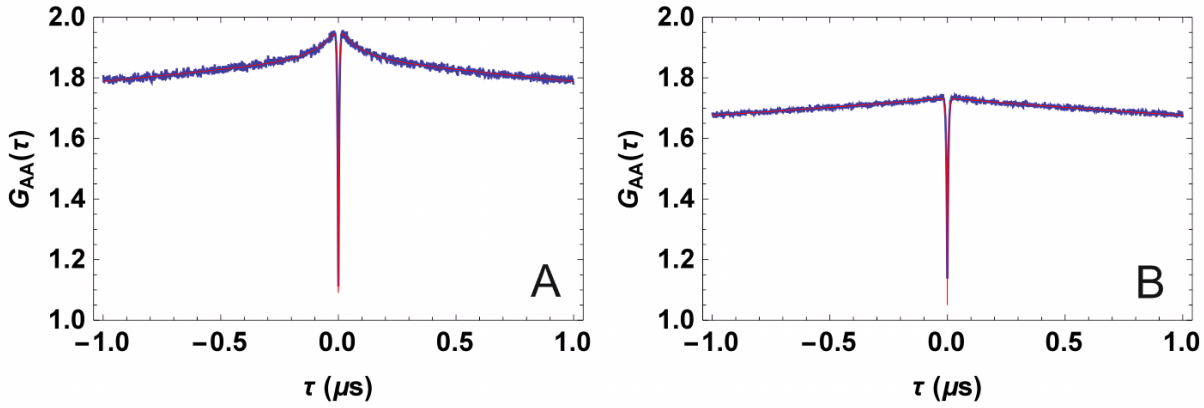


Fig. S4 Nanosecond fluorescence correlation spectroscopy (ns-FCS) data recorded for 1 nM samples of Pro6 (A) and Pro20 (B) peptides terminally (labeled with Alexa 488 (donor) and Alexa 594 (acceptor), Fig. 4) measured in free diffusion in an aqueous buffered solution (50 mM sodium phosphate pH 7.0) with a confocal single-molecule instrument at 295 K (instrumentation and analysis essentially as described previously[6-8]. Shown are the autocorrelations of the acceptor fluorescence emitted upon continuous wave excitation at 488 nm. In both measurements, photon-antibunching (sharp dips around $\tau = 0$) and triplet-blinking (slow decays on the microsecond timescale) are apparent. Most interestingly, however, the Pro6 autocorrelation curve shows a component of positive amplitude decaying on a ~100 ns timescale that is absent in the case of Pro20. Such a component is the expected signature of mutual static contact quenching of the two fluorophores, which in Pro6 are in sufficiently close proximity to form a transient complex given the flexibility of the linkers (Fig. 4a). In Pro20, the dyes are spatially well separated, and interdye-complexes cannot form. The Pro6 correlation data (A) were fit (red curve) with a model function containing three dynamic components (attributed to antibunching, dye-dye quenching, and triplet blinking) of the form $G(\tau) = 1 + a\,(1 - e^{-|\tau|/\tau_{ab}}) \cdot (1 + c_q e^{-|\tau|/\tau_q}) \cdot (1 + c_T e^{-|\tau|/\tau_T})$ . We find for the quenching component $\tau_q = 85\,\text{ns}$. With $\tau_q = 1/\left(k_{on} + k_{off}\right)$ and $c_q = k_{on}/k_{off} = 0.11$,[9] the on- and off-times for dye association and dissociation result as $1/k_{\text{off}} =$ 94 ns and $1/k_{\text{on}} = 0.86$ µs, respectively, corresponding to 10 % of the population in the state where the dyes are associated. The Pro20 data (B) can be fit well with only two components (antibunching and triplet blinking).

[1] B. Nikoobakht and M. A. El-Sayed, "Preparation and growth mechanism of gold nanorods (NRs) using seed-mediated growth method," *Chemistry of Materials,* vol. 15, pp. 1957-1962, May 2003.

[2] H. Yuan, S. Khatua, P. Zijlstra, and M. Orrit, "Individual gold nanorods report on dynamical heterogeneity in supercooled glycerol," *Faraday Discussions,* vol. 167, pp. 515-527, 2013 2013.

[3] R. Zondervan, F. Kulzer, H. van der Meer, J. Disselhorst, and M. Orrit, "Laser-driven microsecond temperature cycles analyzed by fluorescence polarization microscopy," *Biophysical Journal,* vol. 90, pp. 2958-2969, Apr 2006.

[4] H. Yuan, T. Xia, B. Schuler, and M. Orrit, "Temperature-cycle single-molecule FRET microscopy on polyprolines," *Physical Chemistry Chemical Physics,* vol. 13, pp. 1762-1769, 2011 2011.

[5] S. Sindbert, S. Kalinin, H. Nguyen, A. Kienzler, L. Clima, W. Bannwarth*, et al.*, "Accurate distance determination of nucleic acids via Forster resonance energy transfer: implications of dye linker length and rigidity," *J. Am. Chem. Soc.,* vol. 133, pp. 2463-80, Mar 2 2011.

[6] A. Soranno, B. Buchli, D. Nettels, R. R. Cheng, S. Müller-Späth, S. H. Pfeil*, et al.*, "Quantifying internal friction in unfolded and intrinsically disordered proteins with single-molecule spectroscopy," *Proceedings of the National Academy of Sciences,* vol. 109, pp. 17800-17806, October 30, 2012 2012.

[7] D. Nettels, A. Hoffmann, and B. Schuler, "Unfolded protein and peptide dynamics investigated with single-molecule FRET and correlation spectroscopy from picoseconds to seconds," *J Phys Chem B,* vol. 112, pp. 6137-46, May 15 2008.

[8] D. Nettels, I. V. Gopich, A. Hoffmann, and B. Schuler, "Ultrafast dynamics of protein collapse from single-molecule photon statistics," *Proceedings of the National Academy of Sciences,* vol. 104, pp. 2655-2660, February 20, 2007 2007.

[9] *Single Molecule Detection in Solution: Methods and Applications*: Wiley-VCH Verlag GmbH & Co. KGaA, 2003.